Journal of Gastroenterology and Hepatology

JGHF

doi:10.1111/jgh.16737

ORIGINAL ARTICLE - GASTROENTEROLOGY (EXPERIMENTAL)

Partially hydrolyzed guar gum suppresses binge alcohol-induced liver fat accumulation via gut environment modulation in mice

So Morishima,[*,†] Aya Abe,[†] Saki Okamoto,[†] Mahendra P. Kapoor,[†] Masahide Osumi,[‡] Machi Oda,[§] Tsutomu Okubo,[¶] Makoto Ozeki,[*,†] Masahiro Nishio[‡] and Ryo Inoue[§]

*Laboratory of Food Function, Department of Life Sciences, Graduate School of Bioresources, [‡]Laboratory of Nutritional Chemistry, Department of Life Sciences, Graduate School of Bioresources, [¶]Graduate School of Bioresources, Mie University, Tsu, [†]Nutrition Division, Taiyo Kagaku Co. Ltd, Yokkaichi, Mie, [§]Laboratory of Animal Science, Department of Applied Biological Sciences, Faculty of Agriculture, Setsunan University, Hirakata, Osaka, Japan

Key words
alcoholic fatty liver, *Bifidobacterium*, partially hydrolyzed guar gum, short-chain fatty acid, *Streptococcus*.

Accepted for publication 29 August 2024.

Correspondence
So Morishima, Laboratory of Food Function, Department of Life Sciences, Graduate School of Bioresources, Mie University, 1577 Kurimamachiya, Tsu, Mie 514-8507, Japan.
Email: 522d302@m.mie-u.ac.jp

Ryo Inoue, Laboratory of Animal Science, Department of Applied Biological Sciences, Faculty of Agriculture, Setsunan University, Nagaotoge-cho 45-1, Hirakata, Osaka, 573-0101, Japan.
Email: ryo.inoue@setsunan.ac.jp

Declaration of conflict of interest: There were no particular conflicts of interest. However, referring to a potential conflict of interest, SM, AA, SO, MPK, and MO were employed by Taiyo Kagaku Co., Ltd.

Financial support: This study was partially supported by the Taiyo Kagaku Co., Ltd.

Abstract

Alcohol-associated liver disease (ALD), including alcoholic fatty liver, is a serious problem in many countries, and its economic costs to society are enormous. There is evidence indicating the relations between gut environments and liver disease, and thus, improvement of gut environment is expected to be an effective approach for ALD prevention. In this study, we explored the preventive effect of partially hydrolyzed guar gum (PHGG) on ALD focusing on the gut–liver axis. Two weeks of PHGG pre-feeding suppressed the liver fat accumulation in the experimental binge alcohol model mouse. In cecal microbiome, PHGG pre-feeding increased beneficial *Bifidobacterium* with its metabolite acetate concentration and suppressed the alcohol-induced increase in the potential pathobiont *Streptococcus*. PHGG pre-feeding increased colonic gene expression of angiogenin genes, which act as antimicrobial peptides and decreased expression of genes for mast cell protease, which suggests a potential involvement in leaky gut. Correlation network analysis based on evaluated parameters revealed four relations worth noticing. (i) The abundance of *Bifidobacterium* positively correlated with cecal acetate. (ii) Cecal acetate negatively correlated with *Streptococcus* via colonic angiogenin expression. (iii) *Streptococcus* positively correlated with liver fat area. (iv) Cecal acetate had direct negative correlation with liver fat area. Considering these relations comprehensively, acetate produced by *Bifidobacterium* may be a key mediator in ALD prevention; it inhibited growth of potential pathobiont *Streptococcus* and also directly regulated liver lipid metabolism reaching through portal vein. This study demonstrated that regularly intake of PHGG may be effective in reducing the risk of alcoholic fatty liver via gut–liver axis.

Introduction

Alcohol is one of the leading causes of chronic liver disease in industrialized countries.[1] Alcohol-related liver disorders such as fatty liver, hepatitis, and cirrhosis are collectively referred to as alcohol-associated liver disease (ALD).[2] Alcoholic fatty liver, a symptom developed in an early stage of ALD, typically has no subjective symptoms or clinical signs, and thus, it is crucial to prioritize preventive measures against this symptom.[3]

Recently, the relationship between the gut microbiome and liver has been recognized as the gut–liver axis.[4] As a part of this bidirectional communication, the gut epithelial barrier regulates the transmission of metabolites and/or pathogen-associated molecular patterns (PAMPs) from the gut microbiome to the liver.[4–6] Indeed, associations between several liver disorders and the gut microbiome have been documented in various studies.[7–10] Alcohol consumption has been shown to modulate the gut microbiome, which may in turn exacerbate ALD.[11] On the therapeutic side, short-chain fatty acids (SCFA), a typical metabolite produced by gut bacteria, have been reported beneficial for maintenance of gut homeostasis including epithelial barrier function.[12] Furthermore, when SCFA reached to the liver through the portal vein, SCFA promote several metabolic regulation including fat metabolism.[12] Therefore, SCFA is thought to be deeply associated with improvement/prevention of several liver disease.[12,13] In this context, targeted manipulation of the gut microbiome through prebiotics or probiotics is expected to be a promising approach for the suppression of ALD. However, there are limited reports regarding suppressive effects of prebiotics and probiotics, especially the former, with focuses on the gut–liver axis.[14,15] Currently, studies evaluating on the preventive effects

of functional foods on ALD have mainly focused on antioxidant capacity in the liver.[16–19]

Partially hydrolyzed guar gum (PHGG) is a prebiotics used for modulation of gut microbiome in a favorable state to have a health benefit and has been linked to a number of health advantages, including protection against nonalcoholic fatty liver disease (NAFLD).[20–22] There is one study reported suppression of PHGG on experimentally induced ALD in mice. However, that study focused on the direct effects of PHGG on liver, such as antioxidant capacity, and no evaluations on gut functions including microbiome were conducted.[23] Therefore, potential of PHGG on prevention of ALD has not been investigated yet in regard to gut–liver axis. In this study, we assessed the hepatoprotective effect of PHGG under binge alcohol administration with special focuses on gut–liver axis in a mouse model.

Materials and methods

Animal. The animal experiments in the present study were approved by the Ethical Experimental Animal Committee of Mie University (approval number: 2022-7) and carried out in accordance with their guidelines.

Male C57BL/6N mice aged 7 weeks were purchased from Japan SLC (Shizuoka, Japan). The animals were separated into three groups (C: control; A: alcohol; AP: alcohol + PHGG pre-feeding) so that their mean body weights were almost equal and housed three mice in each cage. All animals were kept at a controlled temperature (22 ± 2 °C) and light (turn on at 8:00 and off at 20:00). Water and standard chow (AIN-93G, Oriental Bio-Service, Kyoto, Japan) were available ad libitum during acclimatization. After a week of acclimatization, group AP received modified AIN-93G (5% PHGG instead of 5% cellulose; PHGG is commercially provided by Taiyo Kagaku Co., Ltd., Mie, Japan) in place of standard AIN-93G, and all animals were kept for an additional 2 weeks. After that, a previously established binge alcohol model mouse was conducted, as used in the report by Kim *et al*.[24] Briefly, three doses of ethanol (5 g/kg/dose) were administered orally at 12-h intervals to A and AP groups. Equivalent calories of dextrose solution was given to C group. After an hour of the last administration, the animals were immediately dissected under isoflurane anesthesia. Blood was drawn from the inferior vena cava, and serum was collected using a Separapid tube (Kenis, Osaka, Japan) according to the manufacturer's instructions. The collected serums were stored at −80°C until further analysis. Weight of whole liver was measured, and small pieces (approximately 100 mg) of the biggest liver lobe were collected and stored at −80°C for biochemical analysis. Similar-sized pieces of the biggest liver lobe were cryoembedded in optimal cutting temperature compound (Sakura Finetek Japan Co., Ltd., Tokyo, Japan) for histology and stored at −80°C. The cecal contents were collected for cecal microbiome analysis and for measurement of organic acids concentration and stored at −80°C. Small pieces of colonic tissue were collected for transcriptome analysis and permeated overnight at 4°C in RNAlater solution (Thermo Fisher Scientific, Tokyo, Japan) and then stored at −20°C.

Serum biochemical analysis. Serum aspartate transaminase (AST), alanine transaminase (ALT), triglyceride (TG), and albumin (ALB) assays were outsourced to Oriental Yeast Co., Ltd. (Tokyo, Japan).

Liver fat accumulation analysis. For the biochemical analysis of liver TG, lipids were extracted from small pieces of liver using chloroform and methanol (2:1). Organic solvents were evaporated under the N2 stream and resuspended in isopropanol. LabAssay Triglyceride (Wako, Osaka, Japan) was employed to determine TG concentrations.

For the histological evaluation, oil red O was used to stain 10-μm frozen sections, and hematoxylin was used as a counterstain. A bright-field microscope equipped with a digital camera was used to capture 10 randomly chosen images of hepatocytes for each sample. The ratios of the oil-red O-stained area in each image were estimated from the measured red color area using the software ImageJ2/Fiji (Version 2.9.0).[25]

Cecal microbiome and organic acids. Bacterial DNA extraction from cecal contents, library preparation, sequence using MiSeq (Illumina, Tokyo, Japan), and sequence data analysis were performed according to a previous study.[26] The estimation of cecal organic acid (succinate, lactate, formate, acetate, propionate, *iso*-butyrate, *n*-butyrate, *iso*-valerate, and *n*-valerate) concentrations was also performed using ion-exclusion high-performance liquid chromatography, as previously reported.[26]

Colonic transcriptome analysis. Tissue fragments were removed from RNAlater solution and homogenized in 1 mL of TRIzol (Thermo Fisher Scientific, Tokyo, Japan) using a TissueRuptor (QIAGEN, Tokyo, Japan). RNA was isolated from tissue homogenates using the phenol–chloroform method and purified by the RNeasy mini kit in conjunction with the RNase-Free DNase Set (both from QIAGEN, Tokyo, Japan). The 3′ mRNA library was prepared with a commercially available kit (Collibri 3′ mRNA Library Prep Kit for Illumina Systems, Thermo Fisher Scientific, Tokyo, Japan) following the manufacturer's instructions and that subsequently sequenced on Illumina HiSeq X (Illumina, Tokyo, Japan). Adaptor trimming and quality filtering of raw sequences was performed using Cutadapt (ver. 2.8). Processed sequence was mapped to genome sequence using STAR (ver. 2.7.10a), and transcripts were counted by featureCounts (ver. 2.0.0). The analysis of feature count data was performed using R (ver. 4.2.0) and the edgeR package (ver. 3.38.4). Read counts were normalized using the trimmed mean of M values approach. For the identification and detection of differentially expressed genes (DEG), the likelihood ratio test was used. DEGs were defined as genes with false discovery ratio (FDR) < 0.05 and $|\text{Log 2 fold change}| > 1$. For visualization of each DEG read count, read count data were additionally normalized using the count per million (CPM) approach.

Real-time PCR. Five DEGs were quantified using the reverse transcription qPCR technique to validate the transcriptome data. The same RNA samples utilized in the transcriptome analysis were reverse transcribed by the ReverTra Ace qPCR RT Kit (TOYOBO, Osaka, Japan) according to the manufacturer's instructions. Quantitative PCR was performed using the Roche Light Cycler 96

system (Tokyo, Japan). PowerUp SYBR Green Master Mix (Thermo Fisher Scientific, Tokyo, Japan) was used for intercalation method. Its PCR procedure included 45 cycles of 15 s at 95°C and 60 s at 60°C and 15 s of pre-melt hold at 95°C, followed by an examination of the dissociation curve from 60 to 95°C. Before PCR procedure, the uracil-DNA glycosylase and polymerase were activated for 2 min at 50 and 95°C, respectively. LightCycler 480 Probes Master with Universal Probe Library Set (Roche, Tokyo, Japan, currently unavailable) was used for probe method. Its PCR procedure included 45 cycles of 10 s at 95°C, 30 s at 60°C, and 1 s at 72°C, followed by cooling 10 s at 50°C after PCR cycles. Before PCR procedure, pre-incubate for 10 min at 95°C. The name of DEGs evaluated and sequences for their primers and probe are shown in Table S1 with references [27, 28]. All assays were performed in duplicate. The acquired data were normalized using *Actb* mRNA expression.

Statistical analysis. Unless otherwise noted, all data are provided as means ± SEM. We used Welch's *t*-test to compare two groups. A one-way analysis of variance (ANOVA) followed by Tukey's HSD test were used for multiple group comparisons. The machine learning and calculation of valuable importance process were carried out with the R package randomForest (Version 4.7-1.1), and the area under the ROC curve (AUC) was computed and visualized with the R package pROC (Version 1.18.0). In correlation test, we used Pearson's product–moment correlation or Kendall rank correlation coefficient according to value normality result by Shapiro–Wilk normality test. Unless otherwise noted, all statistical analyses were carried out using R software (Version 4.2.0). The $P < 0.05$ was considered significant.

Correlation network analysis. The correlation network was generated according to the results of correlation test and visualized using the software Cytoscape (ver. 3.9.1). Data from A and AP were applied to focus on suppression of fatty liver but not on effect of binge alcohol. Serum and liver biochemical data, quantified histological data, relative abundances of 15 bacterial genera that extracted by valuable importance analysis of machine learning model, major cecal SCFA concentrations (acetate, *n*-butyrate, propionate), and DEG count data were used for the correlation test. A correlation network was built using the correlation coefficients from significant ($P < 0.05$) relationships.

Table 1 Tissue weights and biochemical parameters

	C (n = 6)	A (n = 6)	AP (n = 6)	P value
Tissue weight				
Body weight (g)	24.25 ± 0.79	23.81 ± 0.61	23.42 ± 0.53	0.679
Liver weight (g)	0.99 ± 0.05	0.92 ± 0.04	1.02 ± 0.04	0.286
Liver/body weight (g)	0.041 ± 0.002	0.039 ± 0.002	0.044 ± 0.001	0.069
Serum biochemical parameters				
AST (IU/L)	220.5 ± 13.74	237.0 ± 27.46	245.8 ± 35.77	0.803
ALT (IU/L)	44.83 ± 9.28	62.17 ± 5.96	54.33 ± 7.75	0.316
TG (μmol/L)	48.00 ± 8.16	73.33 ± 12.40	95.17 ± 16.53	0.061
ALB (g/dL)	2.95 ± 0.09[a]	2.08 ± 0.09[b]	2.05 ± 0.06[b]	<0.001**
Liver biochemical analysis				
Liver TG (mg/g tissue)	11.41 ± 2.90[a]	90.71 ± 7.61[b]	69.44 ± 9.46[b]	<0.001**

**$P < 0.01$ (one-way ANOVA).

Different letters indicate significant differences among groups (Tukey's HSD test, $P < 0.05$).

ALB, albumin; ALT, alanine transaminase; AST, aspartate transaminase; TG, triglyceride.

Results

PHGG suppresses alcohol-induced liver fat accumulation. Table 1 represents tissue weight and biochemical data. There was no significant difference in major serum markers (AST, ALT, and TG) or tissue weight. However, alcohol administration substantially lowered serum ALB.

Regarding fatty liver, alcohol treatment significantly increased the hepatic fat area, and PHGG pretreatment seems suppressed the fat accumulation (Fig. 1a). The results of the image analysis demonstrated significant increase in liver fat area with alcohol treatment (Fig. 1b; group C: 2.89 ± 0.47%, group A: 17.68 ± 1.18%), which was greatly suppressed with PHGG pre-feeding (group AP: 11.87 ± 2.16%). Biochemical examination of liver TG showed a similar pattern to hepatic fat area, but significant difference between A and AP was not found (Table 1).

Gut microbiome and its metabolites affected by both alcohol and PHGG feeding. There was no significant difference in alpha diversity indices of the cecal microbiome (Table S2). However, beta diversity differed significantly between groups, demonstrating that both alcohol administration and PHGG pre-feeding altered microbiome composition (Fig. 2a). At the phylum level, relative abundance of Proteobacteria was significantly increased, and Desulfobacterota was decreased by alcohol treatment in both group A and AP (Table S3). PHGG pretreatment was significantly increased Actinobacteriota and decreased Deferribacteriota.

At the genus level, significant differences were found in 39 genera (Table S4). A random forest approach was used to screen the bacterial genera that might be important in the development and suppression of ALD and successfully divided the cecal microbiome of groups C versus A and A versus AP with 100% precision (AUC = 1.0; Fig. 2b). A variable importance analysis of the prediction model revealed that the abundance of *Streptococcus* was important for the prediction accuracy of learning model for both C versus A and A versus AP comparisons (Fig. 2c). In 15 genera found in the valuable importance analysis of A versus AP, 12 genera were increased by PHGG pre-feeding including *Bifidobacterium* and *Muribaculum*, while three genera, including *Streptococcus* and *Mucispirillum*, were decreased. The relative abundances of some of those bacteria were shown in Figure 2d.

Cecal organic acid concentrations were assessed as typical metabolites from the gut microbiome (Table 2). As one of the SCFA, group AP showed a significantly higher acetate concentration compared to group A. AP group also showed significantly high succinate and low formate concentrations compared to other groups.

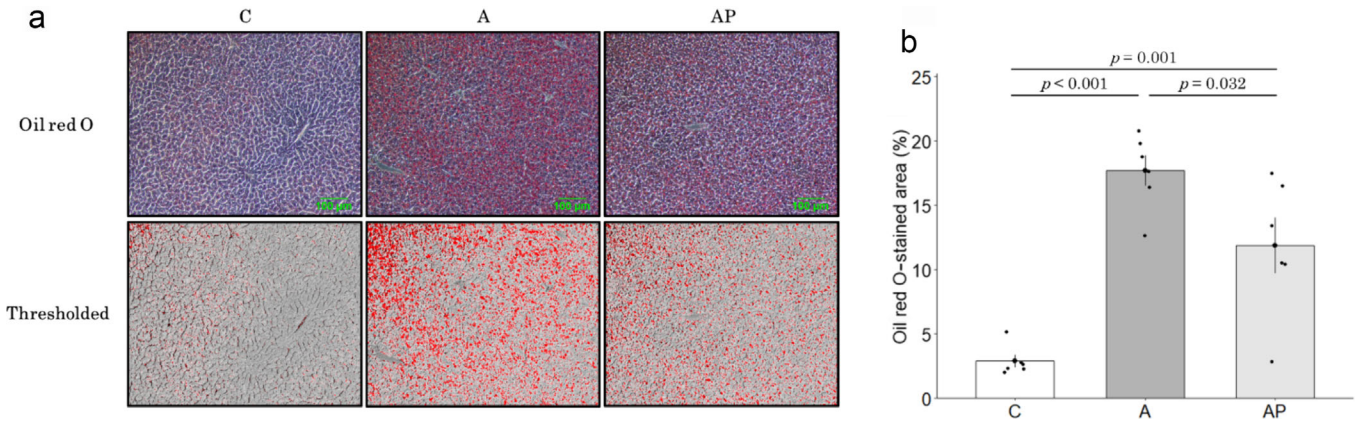

Figure 1 PHGG pre-feeding suppressed binge alcohol-induced liver fat accumulation. (a) Representative oil red O and hematoxylin-stained liver section and its threshold processed fat area using ImageJ2/Fiji software (100×). (b) The ratios of oil red O-stained area in liver section images. Data represent means ± SEM. The significance of the values was determined by Tukey's HSD after a one-way ANOVA.

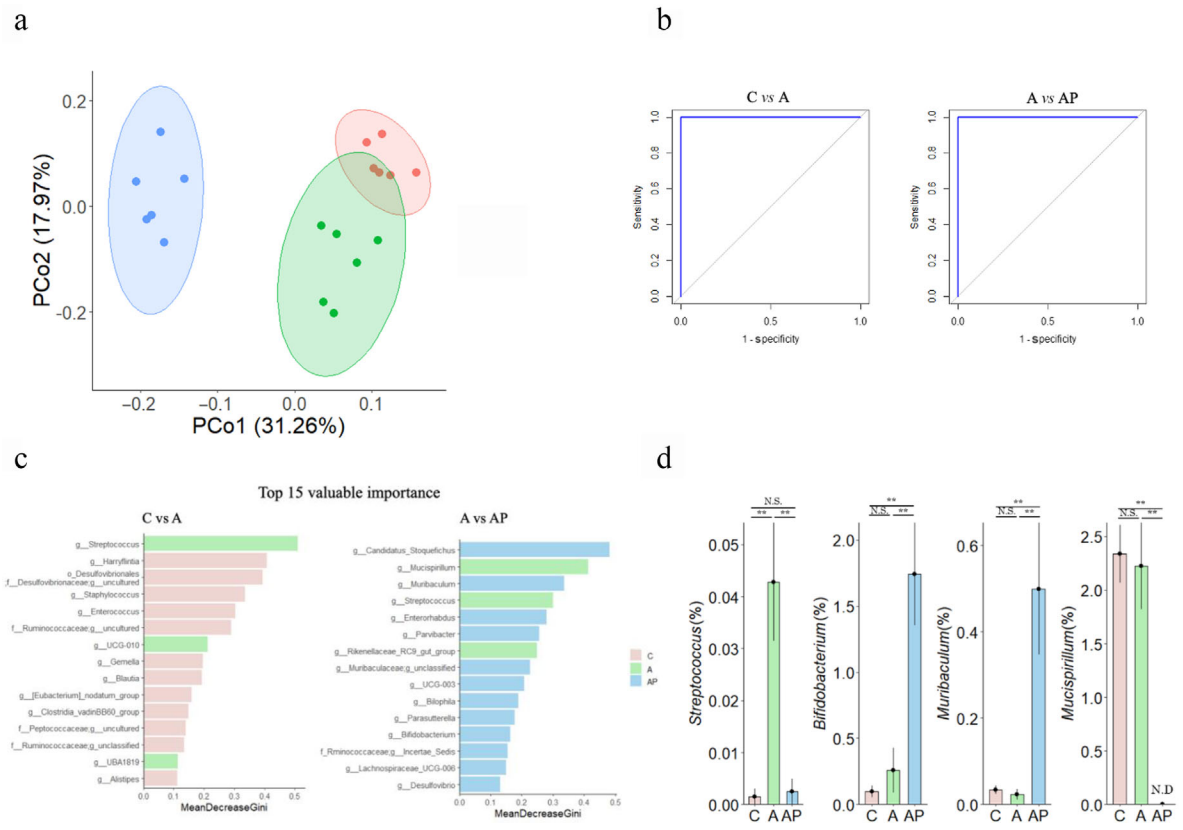

Figure 2 Both binge alcohol and PHGG pre-feeding affected cecal microbiome composition. (a) Principal coordinate analysis (PCoA) of cecal microbiome based on unweighted UniFrac distance. ●, C; ●, A; ●, AP. The ellipse enclosing each cluster indicate a 95% confidence interval. $P < 0.05$ within each group by pairwise permutational analysis of variance (PERMANOVA) test. (b) The ROC curve indicating model precision. (c) The top 15 bacterial relative abundances with the highest valuable importance in the machine learning model of group C versus A and A vs AP comparison using random forest algorithm. The higher the mean decrease Gini, the higher the variable importance in the machine learning model. The filled color of the plot represents the group with the higher abundance of bacteria compared to another group (o, order; f, family; g, genus). (d) Relative abundances of representative bacteria in each group. Data represent means ± SEM. Significance of the values were determined Tukey's HSD after one-way ANOVA. $*P < 0.05$, $**P < 0.01$ between each group.

Table 2 Cecal organic acids

Organic acid (μmol/kg contents)	C (n = 6)	A (n = 6)	AP (n = 6)	P value
Succinate	0.717 ± 0.209[a]	1.743 ± 0.464[a]	4.123 ± 1.482[b]	0.048*
Lactate	ND	1.012 ± 0.689	12.380 ± 9.169	0.220
Formate	1.642 ± 0.247[a]	1.002 ± 0.136[a]	0.602 ± 0.112[b]	0.003**
Acetate	29.637 ± 2.073[ab]	27.208 ± 2.833[a]	36.153 ± 1.298[b]	0.028*
Propionate	5.065 ± 0.671	3.210 ± 0.621	4.855 ± 0.983	0.213
iso-Butyrate	1.187 ± 0.274	2.093 ± 0.553	1.860 ± 0.719	0.494
n-Butyrate	2.135 ± 0.283	1.752 ± 0.354	1.727 ± 0.234	0.560
iso-Valerate	0.117 ± 0.073	0.225 ± 0.084	0.072 ± 0.046	0.303
n-Valerate	0.108 ± 0.041	0.092 ± 0.058	0.068 ± 0.045	0.845
Total organic acid	40.607 ± 3.103[a]	38.332 ± 3.012[a]	61.847 ± 8.424[b]	0.015*

*$P < 0.05$.
**$P < 0.01$ (one-way ANOVA).
Different letters indicate significant differences among groups (Tukey's HSD test, $P < 0.05$).

Colonic transcriptome analysis revealed several gene expressions were regulated by PHGG pre-feeding immediately after binge alcohol administration. In the 3′ mRNA-sequence analysis, one sample in group A was excluded from the analysis due to an aberrant gene expression pattern likely resulting from a technical error (see Fig. S1). According to a multi-group comparison of three groups using likelihood ratio test, 70 genes showed substantially different expressions among three groups (FDR < 0.05). The heat map of those 70 genes suggested that colonic gene expression was largely influenced by alcohol administration rather than PHGG pre-feeding (Fig. 3a). However, six genes exhibited significantly different expression level between groups A and AP (Fig. 3b). Three angiogenin genes (*Ang4*, *Ang5*, *Ang6*) were expressed significantly higher and three genes (*Mcpt1*, *Mcpt2*, *B3galt2*) expressed lower in group AP than group A. These six genes were not considered as DEGs in group C when compared with group A (Fig. 3c). The validation of five genes (*Ang4*, *Ang5*, *B3galt2*, *Mcpt1*, *Mcpt2*) using RT-qPCR revealed the same level of expression as 3′ mRNA-seq (Fig. S2). In this study, authors could not establish proper qPCR primer set for validation of *Ang6*.

Correlation network analysis implicates potential pathways in gut–liver axis. A correlation network was constructed in accordance with the correlation test result using data from groups A and AP, and significant correlations were applied (Fig. 4). One sample in group A was excluded from network analysis because it lacked accurate 3′ mRNA count data as mentioned above. Among the significant correlations used for network construction, the minimum absolute correlation coefficient was 0.60. It is noteworthy that liver fat indicators (liver TG and oil red O-stained area ratio) were negatively correlated with *Bifidobacterium* abundance and the concentration of its usual metabolite acetate. In contrast, there was a positive correlation between liver fat indicators and the abundance of *Streptococcus*. There were several bacteria negatively correlated with mast cell protease (*Mcpt*) expression, but only *Streptococcus* was positively correlated. Angiogenin (*Ang*) with antimicrobial effect was negatively correlated with several bacteria including *Streptococcus*, while there were also several bacteria positively correlated. Cecal acetate also positively correlated with two of angiogenin.

Discussion

In this study, we evaluated prebiotic and hepatoprotective effect of PHGG under binge alcohol administration. To estimate preventative pathways of alcoholic fatty liver via gut–liver axis, gut microbiota and colonic gene expression were evaluated. Also, correlations of gut environment with liver fat were analyzed. The predicted working model for PHGG under binge alcohol administration based on the results obtained is shown in Figure 5.

Most of tissue weight and biochemical parameters were not significantly different between groups indicating that the binge alcohol administration did not seriously impair liver function, with the exception for liver fat accumulation and decrease in serum albumin. Although PHGG administration did not restore serum albumin levels, it prevented liver fat accumulation.

Regarding to the gut microbiome, binge alcohol affected its composition. Since the majority of ethanol is absorbed in the stomach and small intestine, it is difficult to consider that orally administered ethanol directly enters the large intestine. Therefore, ethanol and acetaldehyde from blood flow or modified bowel movements may be the factors of this modification. *Streptococcus* is positively correlated with liver fat, and other studies have reported associations of *Streptococcus* with liver disorders such as severe ALD and with the severity of hepatitis C.[29–31] The mechanism by which *Streptococcus* is involved in the severity of fatty liver could not be clarified in this study, but a link between this bacterium and gut inflammation may be involved. Increase in abundance of *Streptococcus* has been reported in inflammatory bowel disease, and therefore, *Streptococcus* may exacerbate gut inflammation and consequently increased intestinal permeability.[32,33] It can be reasonably deduced that the suppression of increase in this potential pathobiont *Streptococcus* by PHGG pre-feeding may have contributed to the improvement in ALD.

The relationship between alcohol consumption and increased intestinal permeability has been discussed elsewhere.[34–36] Degradation of epithelial tight junction proteins as a result of the action by mast cells,[36] acetaldehyde,[34] or alcohol[37] is a suggested mechanism in the increased intestinal permeability by alcohol. The increased expression of *Mcpt* in this study is in line with this suggestion as its protease activity can degrade tight junction proteins such as occludin and claudin.[38,39] Therefore, low expression of *Mcpt* by PHGG pre-feeding is potentially beneficial to maintain intestinal barrier function. Additionally, the amount of colonic mucin evaluated by periodic acid-Schiff staining technique was not differ among the groups (data not shown), indicating change in mucus layer thickness may not be involved in change in intestinal permeability and beneficial effect of PHGG.

However, no direct assessment of intestinal permeability was conducted in this study; therefore, further investigation including the quantification of tight junction proteins and blood markers such as lipopolysaccharides is required.

Bifidobacterium, which showed a negative correlation with liver fat, is a typical acetate producer, and several studies have reported

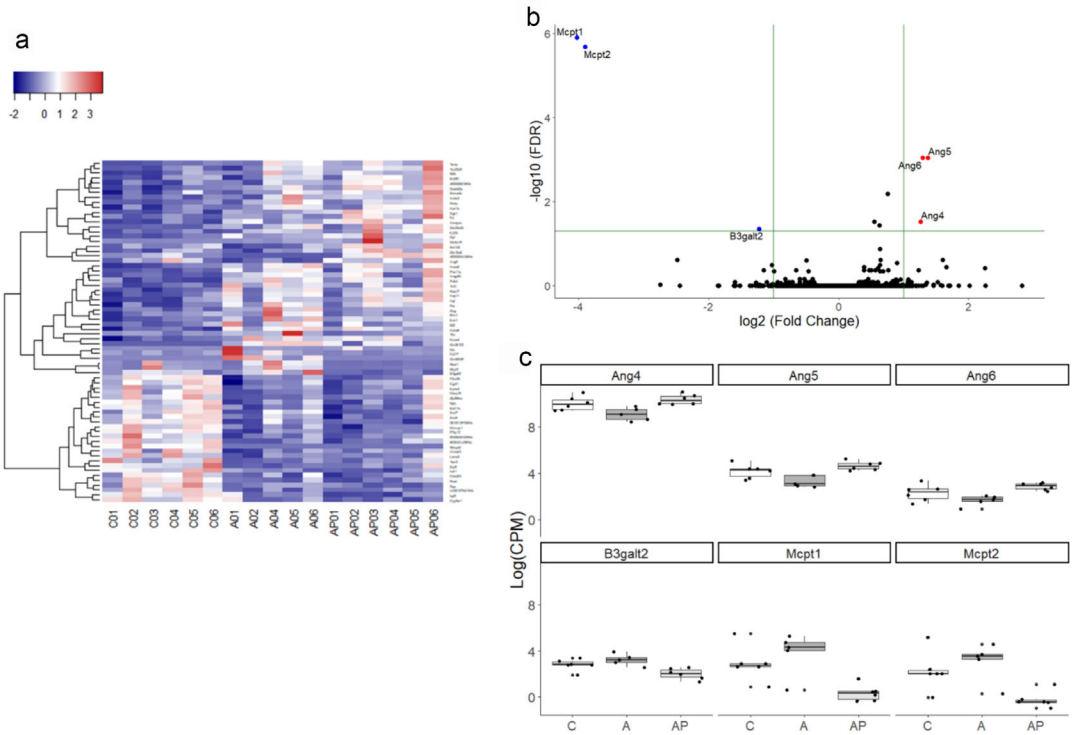

Figure 3 Binge alcohol and PHGG pre-feeding changed transcriptome profiles. (a) The gene heat map shows that those expressions are largely influenced by binge alcohol administration. The significance of the values was determined by multi-group comparison using the likelihood ratio test (FDR < 0.05). (b) Volcano plot comparing gene expression between groups A and AP. DEGs in group AP compared to group A are indicated using red (upregulated) and blue (downregulated) spots. DEGs were defined as genes with false discovery ratio (FDR) < 0.05 and absolute Log 2 fold change >1. (c) The gene counts of DEGs between A and AP groups. Values are additionally normalized using the CPM method.

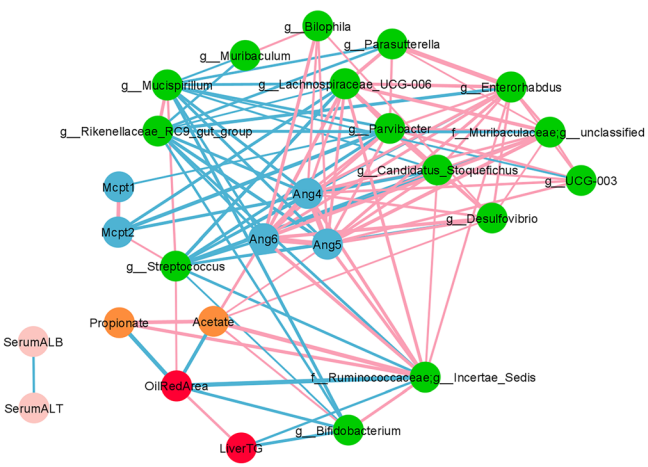

Figure 4 Correlation network analysis. The red edge indicates a positive correlation, and the blue edge indicates a negative correlation, respectively. Each correlation was statistically significant by correlation test ($P < 0.05$, $|r| \geq 0.60$). , Bacteria; , Colonic mRNA expression; , Serum biochemical; , Liver fat; , Cecal organic acid.

an increase of this bacterial genus with PHGG intake.[40,41] The abundance of *Bifidobacterium* positively correlated with cecal acetate concentration and then cecal acetate was positively correlated with the expression of antimicrobial angiogenins. These network connections indicated that the acetate produced by *Bifidobacterium* has an ability to induce expression of angiogenins in the colon. Although SCFA, including acetic acid, have been reported to modulate gene expression in the gut, their effects on angiogenin expression have not been shown.[42] It could be exerted in a specific circumstance such as under the effect of alcohol, and there also be a possibility for acetate to indirectly induce these genes by modulating the abundance of genus unclassified family *Ruminococcaceae*, as this genus positively correlate both with acetate and genes for angiogenins (Fig. 4). The mechanism by which

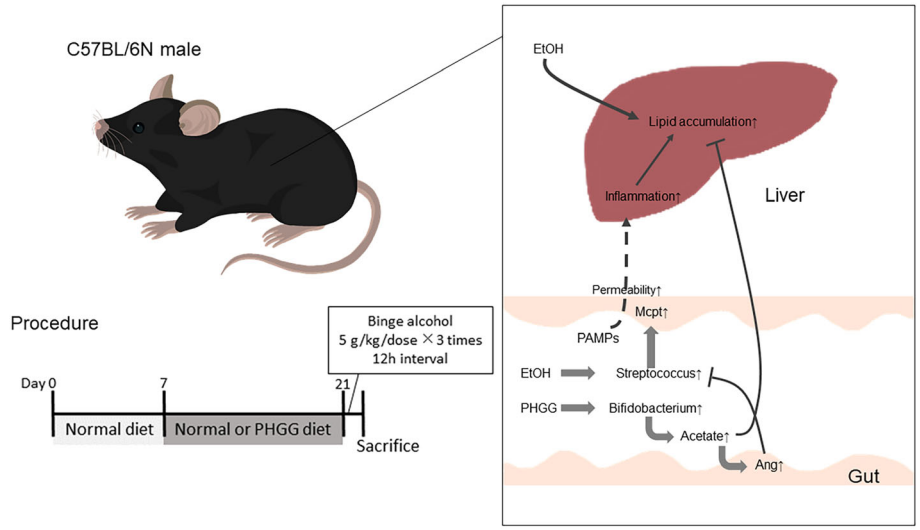

Figure 5 The summary of the present study data and predicted suppression mechanism of alcohol-induced liver fat accumulation by PHGG pre-feeding.

acetate modulates the expression of angiogenins are needed to elucidate further.

Because angiogenins have antimicrobial potentials and expression levels of genes for angiogenins were negatively correlated with *Streptococcus*, angiogenins presumably contributes to the inhibition of growth of *Streptococcus*. There was also a direct negative correlation between *Bifidobacterium* and *Streptococcus*, but the correlation between acetic acid and genes for angiogenins had a larger correlation coefficient than that between *Bifidobacterium* and *Streptococcus*. Therefore, it is assumed that the increase in *Bifidobacterium* suppressed *Streptococcus* indirectly via acetate production and modulation of angiogenins gene expression.

The effect of acetate on the regulation of liver function can also be inferred as another suppressive pathway of liver fat accumulation. Acetate has been reported to have a variety of physiological roles, including the improvement of NAFLD through the suppression of liver fat accumulation.[43–45] Gut-derived acetate is transported to the liver through the hepatic portal vein and is known to have a role as a mediator of metabolism. Several studies have reported the proof that acetate administration lowers liver fat accumulation and suppresses fat synthesis.[43] Therefore, it can be assumed that acetate produced in colon showed a similar effect in this study. Additionally, it is reported previously that intestinal SCFA is lower in ALD patients than healthy individuals.[46] This observation suggests that the supplementation of SCFA may offer a potential benefit to those population.

Involvement of intestinal SCFA receptors, namely, GPR41, GPR43, and GPR109a, in the suppression of liver fat accumulation is unclear in this study.[47,48] The gene expression levels of these receptors did not differ among the groups. However, it is reported that signaling through GPR43 can be archived fairly quick, and it does not always happen with change in gene expression.[49–51] Thus, further investigations such as use of GPR41 or GPR43 KO mice are required to elucidate whether SCFA receptors is involved in phenomenon found in this study.

Studies focused on the relationship between formate and the host physiology are limited, but there are some reports exist indicating increased formate in the blood or intestine is associated with liver disease and inflammatory bowel disease.[52–54] Therefore, the decrease of cecal formate by PHGG pre-feeding may have had positive impact on improving ALD. Succinate has been reported to induce inflammation in the intestine,[55] while there are also reports that it is useful for improving the barrier function by promoting intestinal mucus production and also useful for regulation of fat metabolism.[56,57] Therefore, further study is needed to determine whether the increase of cecal succinate caused by PHGG pre-feeding was involved in suppression of ALD.

The result summarized that PHGG pre-feeding caused a shift to a gut microbiome state especially rich in acetate production. This shift of gut microbiome improved hepatic lipid metabolism and finally inhibited alcohol-induced liver fat accumulation (Fig. 5).

Conclusion

In this study, we exploratory investigated the potential hepatoprotective mechanism of PHGG from binge alcohol-induced ALD via gut–liver axis. Excessive alcohol consumption results in fatty liver and changes in unfavorable gut microbiome composition. PHGG pre-feeding drove the shift of gut microbiome to a state rich in acetate production and inhibited the growth of potential pathobiont *Streptococcus*, a bacteria suggested to be associated with onset of ALD. Increase in colonic angiogenin expression brought by intestinal acetate may be involved in this effect. Suppression of colonic *Mcpt* expression and increases in cecal acetate by PHGG pre-feeding may have positively affected on intestinal barrier function and may be involved as a mechanism for ALD suppression. Furthermore, gut-derived acetate should also regulate liver lipid metabolism and contributes to suppress liver fat accumulation. This study implies that regularly intake PHGG may be effective in preventing ALD through gut–liver axis.

References

1 Rocco A, Compare D, Angrisani D, Sanduzzi Zamparelli M, Nardone G. Alcoholic disease: liver and beyond. *World J. Gastroenterol.* 2014; **20**: 14652–9.
2 Seitz HK, Bataller R, Cortez-Pinto H *et al*. Alcoholic liver disease. *Nat. Rev. Dis. Primers* 2018; **4**: 16.
3 Torruellas C, French SW, Medici V. Diagnosis of alcoholic liver disease. *World J. Gastroenterol.* 2014 Sep; **20**: 11684–99.
4 Albillos A, De Gottardi A, Rescigno M. The gut-liver axis in liver disease: pathophysiological basis for therapy. *J. Hepatol.* 2020; **72**: 558–77.
5 Koh A, De Vadder F, Kovatcheva-Datchary P, Bäckhed F. From dietary fiber to host physiology: short-chain fatty acids as key bacterial metabolites. *Cell* 2016; **165**: 1332–45.
6 Weiss GA, Hennet T. Mechanisms and consequences of intestinal dysbiosis. *Cell. Mol. Life Sci.* 2017; **74**: 2959–77.
7 Safari Z, Gérard P. The links between the gut microbiome and non-alcoholic fatty liver disease (NAFLD). *Cell. Mol. Life Sci.* 2019; **76**: 1541–58.
8 Chopyk DM, Grakoui A. Contribution of the intestinal microbiome and gut barrier to hepatic disorders. *Gastroenterology* 2020; **159**: 849–63.
9 Tilg H, Adolph TE, Trauner M. Gut-liver axis: pathophysiological concepts and clinical implications. *Cell Metab.* 2022; **34**: 1700–18.
10 Chen B, Huang H, Pan CQ. The role of gut microbiota in hepatitis B disease progression and treatment. *J. Viral Hepat.* 2022; **29**: 94–106.
11 Meroni M, Longo M, Dongiovanni P. Alcohol or gut microbiota: who is the guilty? *Int. J. Mol. Sci.* 2019; **20**: 4568.
12 Portincasa P, Bonfrate L, Vacca M *et al*. Gut microbiota and short chain fatty acids: implications in glucose homeostasis. *Int. J. Mol. Sci.* 2022; **23**: 1105.
13 Chen J, Vitetta L. Gut microbiota metabolites in NAFLD pathogenesis and therapeutic implications. *Int. J. Mol. Sci.* 2020; **21**: 5214.
14 Wang Z, Zhang X, Zhu L *et al*. Inulin alleviates inflammation of alcoholic liver disease via SCFAs-inducing suppression of M1 and facilitation of M2 macrophages in mice. *Int. Immunopharmacol.* 2020; **78**: 106062.
15 Yang Y, Liu S, Li H *et al*. The protective effect of *NOSTOC COMMUNE* Vauch. polysaccharide on alcohol-induced acute alcoholic liver disease and gut microbiota disturbance in mice. *J. Gastroenterol. Hepatol.* 2023: jgh.16335.
16 Song Z, Deaciuc I, Song M *et al*. Silymarin protects against acute ethanol-induced hepatotoxicity in mice. *Alcohol. Clin. Exp. Res.* 2006; **30**: 407–13.
17 Oliva J, Bardag-Gorce F, Tillman B, French SW. Protective effect of quercetin, EGCG, catechin and betaine against oxidative stress induced by ethanol in vitro. *Exp. Mol. Pathol.* 2011; **90**: 295–9.
18 Zhao H, Liu S, Zhao H *et al*. Protective effects of fucoidan against ethanol-induced liver injury through maintaining mitochondrial function and mitophagy balance in rats. *Food Funct.* 2021; **12**: 3842–54.
19 Wang M, Zhu P, Jiang C, Ma L, Zhang Z, Zeng X. Preliminary characterization, antioxidant activity in vitro and hepatoprotective effect on acute alcohol-induced liver injury in mice of polysaccharides from the peduncles of *Hovenia dulcis*. *Food Chem. Toxicol. Int. J. Publ. Br. Ind. Biol. Res. Assoc.* 2012; **50**: 2964–70.
20 Takayama S, Katada K, Takagi T *et al*. Partially hydrolyzed guar gum attenuates non-alcoholic fatty liver disease in mice through the gut-liver axis. *World J. Gastroenterol.* 2021; **27**: 2160–76.
21 Takagi T, Naito Y, Higashimura Y *et al*. Partially hydrolysed guar gum ameliorates murine intestinal inflammation in association with modulating luminal microbiota and SCFA. *Br. J. Nutr.* 2016; **116**: 1199–205.
22 Hung TV, Suzuki T. Dietary fermentable fibers attenuate chronic kidney disease in mice by protecting the intestinal barrier. *J. Nutr.* 2018; **148**: 552–61.
23 Wu C, Liu J, Tang Y, Li Y, Yan Q, Jiang Z. Hepatoprotective potential of partially hydrolyzed guar gum against acute alcohol-induced liver injury in vitro and vivo. *Nutrients* 2019; **11**: 963.
24 Kim DH, Sim Y, Hwang JH *et al*. Ellagic acid prevents binge alcohol-induced leaky gut and liver injury through inhibiting gut dysbiosis and oxidative stress. *Antioxidants* 2021; **10**: 1386.
25 Schindelin J, Arganda-Carreras I, Frise E *et al*. Fiji: an open-source platform for biological-image analysis. *Nat. Methods* 2012; **9**: 676–82.
26 Abe A, Morishima S, Kapoor MP *et al*. Partially hydrolyzed guar gum is associated with improvement in gut health, sleep, and motivation among healthy subjects. *J. Clin. Biochem. Nutr.* 2023; **72**: 189–97.
27 Krysko O, Korsakova D, Teufelberger A *et al*. Differential protease content of mast cells and the processing of IL-33 in *Alternaria alternata* induced allergic airway inflammation in mice. *Front. Immunol.* 2023; **19**: 1040493.
28 Cao N, Li JK, Rao YQ *et al*. A potential role for protein palmitoylation and zDHHC16 in DNA damage response. *BMC Mol. Biol.* 2016; **17**: 12.
29 Llopis M, Cassard AM, Wrzosek L *et al*. Intestinal microbiota contributes to individual susceptibility to alcoholic liver disease. *Gut* 2016; **65**: 830–9.
30 Zhong X, Cui P, Jiang J *et al*. *Streptococcus*, the predominant bacterium to predict the severity of liver injury in alcoholic liver disease. *Front. Cell. Infect. Microbiol.* 2021; **17**: 649060.
31 Inoue T, Nakayama J, Moriya K *et al*. Gut dysbiosis associated with hepatitis C virus infection. *Clin. Infect. Dis.* 2018; **67**: 869–77.
32 Teitelbaum JE, Triantafyllopoulou M. Inflammatory bowel disease and *Streptococcus bovis*. *Dig. Dis. Sci.* 2006; **51**: 1439–42.
33 Kojima A, Nomura R, Naka S, Okawa R, Ooshima T, Nakano K. Aggravation of inflammatory bowel diseases by oral streptococci. *Oral Dis.* 2014; **20**: 359–66.
34 Fujimoto Y, Kaji K, Nishimura N *et al*. Dual therapy with zinc acetate and rifaximin prevents from ethanol-induced liver fibrosis by maintaining intestinal barrier integrity. *World J. Gastroenterol.* 2021; **27**: 8323–42.
35 Bode C, Kugler V, Bode JC. Endotoxemia in patients with alcoholic and non-alcoholic cirrhosis and in subjects with no evidence of chronic liver disease following acute alcohol excess. *J. Hepatol.* 1987; **4**: 8–14.
36 Ferrier L, Bérard F, Debrauwer L *et al*. Impairment of the intestinal barrier by ethanol involves enteric microflora and mast cell activation in rodents. *Am. J. Pathol.* 2006; **168**: 1148–54.
37 Bishehsari F, Magno E, Swanson G *et al*. Alcohol and gut-derived inflammation. *Alcohol Res.* 2017; **38**: 163–71.
38 Bramhall M, Zaph C. Mastering gut permeability: new roles for old friends. *Eur. J. Immunol.* 2017; **47**: 236–9.
39 Sorobetea D, Holm JB, Henningsson H, Kristiansen K, Svensson-Frej M. Acute infection with the intestinal parasite *Trichuris muris* has long-term consequences on mucosal mast cell homeostasis and epithelial integrity. *Eur. J. Immunol.* 2017; **47**: 257–68.
40 Sakakida T, Ishikawa T, Doi T *et al*. Water-soluble dietary fiber alleviates cancer-induced muscle wasting through changes in gut microenvironment in mice. *Cancer Sci.* 2022; **113**: 1789–800.
41 Yasukawa Z, Inoue R, Ozeki M *et al*. Effect of repeated consumption of partially hydrolyzed guar gum on fecal characteristics and gut microbiota: a randomized, double-blind, placebo-controlled, and parallel-group clinical trial. *Nutrients* 2019; **11**: 2170.
42 Tan J, McKenzie C, Potamitis M, Thorburn AN, Mackay CR, Macia L. The role of short-chain fatty acids in health and disease. *Adv. Immunol.* 2014; **121**: 91–119.

43 Hernández MAG, Canfora EE, Jocken JWE, Blaak EE. The short-chain datty acid acetate in body weight control and insulin sensitivity. *Nutrients* 2019; **11**: 1943.
44 Kondo T, Kishi M, Fushimi T, Kaga T. Acetic acid upregulates the expression of genes for fatty acid oxidation enzymes in liver o suppress body fat accumulation. *J. Agric. Food Chem.* 2009; **57**: 5982–6.
45 Aoki R, Onuki M, Hattori K *et al*. Commensal microbe-derived acetate suppresses NAFLD/NASH development via hepatic FFAR2 signalling in mice. *Microbiome* 2021; **9**: 188.
46 Baltazar-Díaz TA, González-Hernández LA, Aldana-Ledesma JM *et al*. *Escherichia/Shigella*, SCFAs, and metabolic pathways—the triad that orchestrates intestinal dysbiosis in patients with decompensated alcoholic cirrhosis from western Mexico. *Microorganisms* 2022; **10**: 1231.
47 Lee DH, Kim MT, Han JH. GPR41 and GPR43: from development to metabolic regulation. *Biomed Pharmacother Biomedecine Pharmacother.* 2024; **175**: 116735.
48 Jin C, Chen H, Xie L, Zhou Y, Liu LL, Wu J. GPCRs involved in metabolic diseases: pharmacotherapeutic development updates. *Acta Pharmacol. Sin.* 2024; **45**: 1321–36.
49 Yajima T, Inoue R, Yajima M *et al*. The G-protein on cholesterol-rich membrane microdomains mediates mucosal sensing of short- chain fatty acid and secretory response in rat colon. *Acta Physiol.* 2011; **203**: 381–9.
50 Lu Y, Fan C, Li P, Lu Y, Chang X, Qi K. Short chain fatty acids prevent high-fat-diet-induced obesity in mice by regulating G protein-coupled receptors and gut microbiota. *Sci. Rep.* 2016; **6**: 37589.
51 Hu S, Kuwabara R, De Haan BJ, Smink AM, De Vos P. Acetate and butyrate improve β-cell metabolism and mitochondrial respiration under oxidative stress. *Int. J. Mol. Sci.* 2020; **21**: 1542.
52 Thing M, Werge MP, Kimer N *et al*. Targeted metabolomics reveals plasma short-chain fatty acids are associated with metabolic dysfunction-associated steatotic liver disease. *BMC Gastroenterol.* 2024; **24**: 43.
53 Sun S, Araki Y, Hanzawa F *et al*. High sucrose diet-induced dysbiosis of gut microbiota promotes fatty liver and hyperlipidemia in rats. *J. Nutr. Biochem.* 2021; **93**: 108621.
54 Jia Q, Zhang L, Zhang J *et al*. Fecal microbiota of diarrhea-predominant irritable bowel syndrome patients causes hepatic inflammation of germ-free rats and berberine reverses it partially. *Biomed. Res. Int.* 2019; **2019**: 4530203.
55 Wei YH, Ma X, Zhao JC, Wang XQ, Gao CQ. Succinate metabolism and its regulation of host-microbe interactions. *Gut Microbes* 2023; **15**: 2190300.
56 Kajiwara-Kubota M, Uchiyama K, Asaeda K *et al*. Partially hydrolyzed guar gum increased colonic mucus layer in mice via succinate-mediated MUC2 production. *Npj Sci Food.* 2023; **7**: 10.
57 Li X, Huang G, Zhang Y *et al*. Succinate signaling attenuates high-fat diet-induced metabolic disturbance and intestinal barrier dysfunction. *Pharmacol. Res.* 2023; **194**: 106865.

Supporting information

Additional supporting information may be found online in the Supporting Information section at the end of the article.

Table S1. Primers and probe sequences.
Table S2. Alpha diversity indices of cecal microbiome.
Table S3. Bacterial relative abundances at phylum level.
Figure S1. G7 in group A showed aberrant gene expression pattern indicating technical error. Significantly different expression genes in ANOVA-like test using likelihood test were selected to generate heat map.
Figure S2. Transcriptome data was validated by RT-qPCR. Fold change of five DEGs were shown same trends in both analysis methods. Significance of qPCR data between group A and AP was determined using Whelch's t-test.